Journal of the Nigerian Association of Mathematical Physics
Volume **18 (May, 2011), pp 549 – 554**

Analysis of Tube Drawing Process – A Finite Element Approach

Oladeinde, M.H And Akpobi. J.A

Department of Production Engineering,
Faculty of Engineering,
University of Benin.

Abstract

In this paper the effect of die semi angle on drawing load in cold tube drawing has been investigated numerically using the finite element method. The equation governing the stress distribution was derived and solved using Galerkin finite element method. An isoparametric formulation for the governing equation was utilized along with C^0 cubic isoparametric element. Numerical experimentation showed that the results obtained using the present method is admirable close to the analytical solution and more accurate than finite difference solution. Having established the accuracy of the present solution method, parametric studies were carried out to show the effect of die semi angle on the drawing load for different tube drawing processes. The analysis was carried out using a Visual Basic.Net program developed by the authors. The results are presented in both graphical and tabular forms.

1 Introduction:

Traditionally, the design of good quality products with excellent surface finish has been based on the method of trial and error drawing on extensive experience on the part of the designer. In recent years however, rapid improvement in computing technology has changed this practice. The increasing use of numerical methods for simulating cold forming processes has been observed resulting in reduction of lead times and elimination of trial and error as well as the production of defects free products. Numerical simulation of manufacturing processes has become in the last years an important tool to improve drawing processes, reducing lead times and try out, and providing products free of defects and with controlled mechanical properties [1]

Alexandrova [2] used an upper-bound analysis to estimate the required power in tube drawing and ironing of rigid, perfectly plastic material through a conical die. The frictional stresses exerted by the die and the mandrel on the material have constant values.

Bihamta et al [3] presented a numerical study done on the drawing tubes with variable thickness. The influence of process variables on material thinning and formability in 63.5mm outer diameter, 2.62 mm wall thickness AA6063 aluminum alloy tube, were investigated and optimized. Fisher and Day [4] carried out a study of the factors affecting the tube sinking process using an ABACUS based finite Element program. Panhwar et al [5] formulated a mathematical model for the die-less tube sinking process based on non Newtonian characteristics of the fluid medium and applied a finite-difference numerical technique to solve the governing equations

In this work, tube drawing processes with a plug and mandrel are analyzed numerically using the finite element method. The stress distribution in the tube during the drawing operation is first obtained and subsequently, the effect of die angle on the drawing load is obtained.

Nomenclature

μ_1	Friction coefficient between tube and die wall
μ_2	Friction coefficient between tube and plug
α	semi die angle of the die
β	semi die angle of the plug
D	diameter ot tube
P_1	pressure on the die
P_2	pressure on the plug
h	thickness of tube
σ_0	yield stress

Corresponding authors: ***Oladeinde, M.H***: E-mail: -, Tel. +2348039206421

MATHEMATICAL FORMULATION

Figure 1 presents a scheme of the tube drawing process. A differential element of the tube placed between the die and the plug is represented along with the stresses acting on it as shown in figure 2. Supposing that the process takes place under plain strain conditions ($h << D$ and $D \approx constant$) and that the

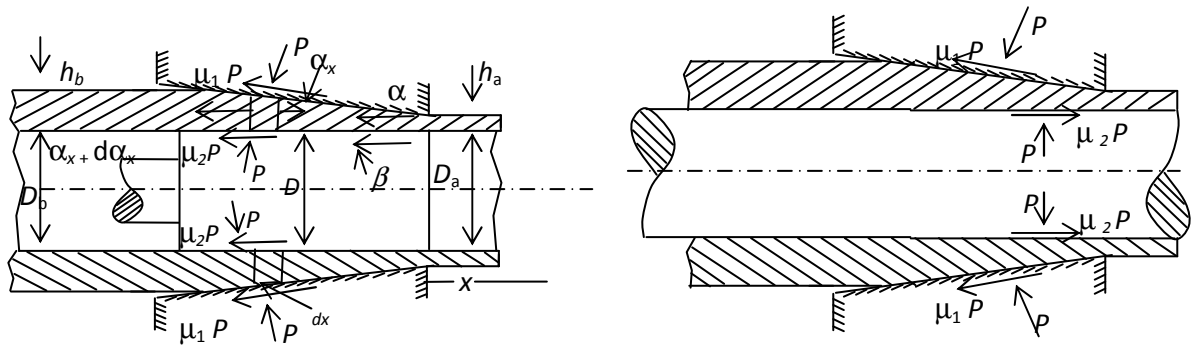

(a) (b)

Figure 1: A schematic diagram of the tube drawing process (a) with slightly tapered plug (b) with a moving mandrel

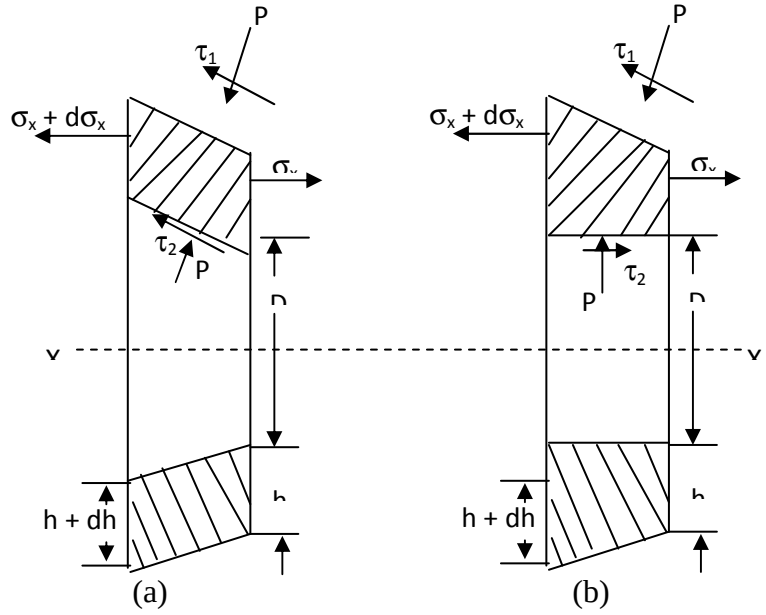

Figure 2: Diagram showing stresses acting on a differential element during tube drawing. (a) with slightly tapered plug (b) with a moving mandrel

pressure on the die, p_1 is equal to the pressure on the plug p_2 and of value, p, then the force balance provides the equation

$$(\sigma_x dh + h d\sigma_x)\pi D + p\pi D(\tan\alpha - \tan\beta)dx + p\pi D(\mu_1 + \mu_2)dx = 0 \quad (1)$$

The decrease in thickness as the element moves through a distance dx is given by (2)

$$dh = dx(\tan\alpha - \tan\beta) \quad (2)$$

Substituting (2) into (1) and simplifying, (3) we obtain

$$(\sigma_x dh + h d\sigma_x) + p.dh\left[1 + \frac{\mu_1 + \mu_2}{\tan\alpha - \tan\beta}\right] = 0 \quad (3)$$

Equation (3) can be rewritten as (5) by noting (4a) which represents the value of B for a tube drawing process with a conical plug. For a cylindrical plug, the value of β equals 0. For a tube drawing process with a moving mandrel the parameter B is computed using (4b)

$$B = \frac{\mu_1 + \mu_2}{\tan\alpha - \tan\beta} \quad (4a)$$

$$B = \frac{\mu_1 - \mu_2}{\tan\alpha - \tan\beta} \tag{4b}$$

$$hd\sigma_x + dh\left[\sigma_x + p\left(1+B\right)\right] = 0 \tag{5}$$

Principal stresses are given by (6) approximately and Tresca's Yield condition is given by

$$\sigma_1 = \sigma_x, \sigma_2 = \sigma_3 = -p \tag{6}$$

$$\sigma_x + p = \sigma_0 \tag{7}$$

Equation 5 can now be written as (8) which is the governing equation for the tube drawing process by using (7).

$$\frac{d\sigma_x}{B\sigma_x - \sigma_0\left(1+B\right)} = \frac{dh}{h} \tag{8}$$

FINITE ELEMENT MODEL

The governing equation in (8) can be re written as

$$\frac{\mathrm{d}\sigma_x}{\mathrm{d}h} - \frac{\mathrm{B}\sigma_x}{\mathrm{h}} - \frac{\sigma_0\left(1+\mathrm{B}\right)}{\mathrm{h}} = 0 \tag{9}$$

Multiplying the modified governing equation (9) by a weight function w_i and integrating over the tube, we obtain

$$\int_0^1\int_0^{2\pi}\int_{D_a}^{D_b} w_i\left(\frac{\mathrm{d}\sigma_x}{\mathrm{d}h} - \frac{\mathrm{B}\sigma_x}{\mathrm{h}} - \frac{\sigma_x\left(1+\mathrm{B}\right)}{\mathrm{h}}\right)\mathrm{d}h\,\mathrm{d}\theta\,\mathrm{d}x = 0 \qquad i = 1, 2....n \tag{10}$$

Equation (10) can be simplified to give

$$2\pi\int_{D_a}^{D_b} w_i\left(\frac{\mathrm{d}\sigma_x}{\mathrm{d}h} - \frac{\mathrm{B}\sigma_x}{\mathrm{h}} - \frac{\sigma_0\left(1+\mathrm{B}\right)}{\mathrm{h}}\right)\mathrm{d}h = 0 \tag{11}$$

$$\int_{D_a}^{D_b} w_i\frac{\mathrm{d}\sigma_x}{\mathrm{d}h}\mathrm{d}h - \int_{D_a}^{D_b} w_i\frac{\mathrm{B}\sigma_x}{\mathrm{h}}\mathrm{d}h - \int_{D_a}^{D_b} w_i\frac{\sigma_0\left(1+\mathrm{B}\right)}{\mathrm{h}}\mathrm{d}h = 0 \tag{12}$$

Where (h_a , h_b) is the domain of the element along the radial direction.

The stress acting on an element can be approximated using (13) from which (14) can be obtained

$$\sigma_x\left(\mathrm{h}\right) = \sum_{j=1}^{n}\sigma_j^e\psi_j^e(\mathrm{h}) \tag{13}$$

$$\frac{\mathrm{d}\sigma_x}{\mathrm{d}h} = \sum_{j=1}^{n}\sigma_j^e\frac{\mathrm{d}\psi_j^e(\mathrm{h})}{\mathrm{d}h} \tag{14}$$

In (13) and (14), ψ_j^e is known as the interpolation function. Setting the weight function equal to the interpolation function, (12) can be rewritten as shown in (15).

$$\int_{h_a}^{h_b}\left[\sigma_j^e\sum_{j=1}^{n}\psi_i^e(\mathrm{h})\mathrm{h}\frac{\mathrm{d}\psi_j^e}{\mathrm{d}h} - \mathrm{B}\sigma_j^e\sum_{j=1}^{n}\psi_i^e\psi_j^e(\mathrm{h})\right]\mathrm{d}h - \int_{h_a}^{h_b}\sigma_0\left(1+\mathrm{B}\right)\psi_i^e\left(\mathrm{h}\right)\mathrm{d}h = 0 \tag{15}$$

Equation (15) can be re written as shown in (16) which represent the finite element model for the tube drawing governing equation.

$$\sum_{j=1}^{n}\int_{h_a}^{h_b}\left[\psi_i^e(\mathrm{h})\mathrm{h}\frac{\mathrm{d}\psi_j^e}{\mathrm{d}h} - \mathrm{B}\psi_i^e\psi_j^e(\mathrm{h})\right]\sigma_j^e = \int_{h_a}^{h_b}\sigma_0\left(1+\mathrm{B}\right)\psi_i^e\left(\mathrm{h}\right)\mathrm{d}h \tag{16}$$

In matrix form, the finite element model can be written as shown in (17)

$$\left\{K_{ij}^e\right\}\left\{\sigma_j^e\right\} = \left\{F_i^e\right\} \tag{17}$$

$\left\{K_{ij}^e\right\}$ is known as the stiffness matrix, $\left\{F_i^e\right\}$ is called the load vector, and $\left\{\sigma_j^e\right\}$ the nodal degree of freedom which is the stress in the wire

Solution Methodology

The domain of the wire under plastic deformation is divided into a number of finite elements. Elemental equations are developed by numerically integrating the weak form of the governing equation shown in (16) using three gauss points four gauss points for C^0 cubic isoparametric elements. This gauss quadrature rule provides sufficient accuracy for the integrals

without incurring unnecessary computing time and resources. The expression for the stiffness matrix shown in (16) are cast in the parent form and to make it solvable using the proposed quadrature method, the parent elements are mapped to the real elements. Equation (18) is the resulting expression for the stiffness matrix and load vectors after the transformation

$$\left[K^{e}\right]=\int_{-1}^{1}\left[\psi_{i}^{e}(\xi)h(\xi)\frac{d\psi_{j}^{e}(\xi)}{d\xi}\frac{1}{J^{e}}+Y(1+B)(\psi_{i}^{e}(\xi)\psi_{j}^{e}(\xi))\right]J^{e}(\xi)d(\xi) \tag{18}$$

The expression for the load vector is given by

$$\left\{F_{i}^{e}\right\}=\int_{1}^{-1}\left[\psi_{i}^{e}(\xi)(\sigma_{0}+B)\right]J^{e}(\xi)d(\xi) \tag{19}$$

In (17) and (18), J^e is known as the jacobian of the element computed using the expression shown in (20)

$$J^{e}=\sum_{j=1}^{n}D_{J}(\xi)\frac{d\psi_{j}}{d\xi} \tag{20}$$

The element stiffness integral and load vectors are evaluated iteratively using a number of preselected Gauss points and weights according to the expression

$$\int_{-1}^{+1}I(\xi)d\xi\simeq\sum_{l=1}^{n}w_{nl}I(\xi_{nl}) \tag{21}$$

The respective element stiffness matrices are assembled by enforcing continuity of nodal stresses. The boundary condition imposed is that there is no longitudinal stress at the entry with no back pull. The interpolation functions for C^0 cubic isoparametric elements are given by

$$\psi_{1}(\xi)=\frac{-9}{16}\left(\xi+\frac{1}{3}\right)\left(\xi-\frac{1}{3}\right)(\xi-1),\quad \psi_{2}(\xi)=\frac{27}{16}(\xi+1)\left(\xi-\frac{1}{3}\right)(\xi-1)$$

$$\psi_{3}(\xi)=\frac{-27}{16}(\xi+1)\left(\xi+\frac{1}{3}\right)(\xi-1),\quad \psi_{4}(\xi)=\frac{9}{16}(\xi+1)\left(\xi+\frac{1}{3}\right)\left(\xi-\frac{1}{3}\right) \tag{22}$$

Numerical Results and Discussion

In order to employ the proposed method developed in the preceding sections for determining the effect of the die semi angle on the drawing load, the accuracy of the solution method is first established. The analytical solution to the tube drawing process shown in (9) assuming elasto plastic model is known and hence comparison can be made. The solution obtained using the present method using increasing mesh density for C^0 cubic isoparametric elements and the analytical solution is shown in Table 1. The values of the parameters used for the simulation are $\mu_1 = 0.15$, $\mu_2 = 0.18$, $\alpha = 14^0$, $\beta = 10^0$, σ_0=1.4KN/mm^2

Table 1: Results obtained using C^0 cubic isoparametric elements, finite difference, and the exact solution.

Location (D)mm	Stress (N/mm^2) 3 elements C^0 cubic	Stress (N/mm^2) 6 elements C^0 cubic	Finite Difference Solution using 10 grid points	Stress (N/mm^2) Exact
1.000000	1.436200	1.436202	1.436202	1.436202
1.055556	1.360479	1.360478	1.357776	1.360479
1.111111	1.269343	1.269349	1.268742	1.269350
1.166667	1.160701	1.160691	1.158441	1.160691
1.222222	1.032203	1.032210	1.031412	1.032211
1.277778	0.881440	0.881445	0.879696	0.881445
1.333333	0.705749	0.705754	0.705149	0.705754
1.388889	0.502310	0.502317	0.501275	0.502318
1.444444	0.268117	0.268130	0.268135	0.268131

The results obtained for different meshes of C^0 cubic isoparametric elements are shown in Table 1 along with finite difference results. The table shows that for a mesh of 6 cubic isoparametric elements, the finite element solution is admirably close to the exact. In particular, the solution converges completely at locations with diameter 1.00000, 1.166667, 1.277778 and 1.33333. At all other points; the error in the finite element solution using 6 cubic isoparametric elements is 0.000001. Pointwise comparison of the errors shows that globally the finite element solution for a mesh of six cubic elements is more accurate than a 10 grid point finite difference solution with a maximum error of 0.000001 obtained for the finite element method compared to 0.002703 for the finite difference method.

Parametric Studies

The C^0 cubic isoparametric element has been shown to produce fairly accurate results for the tube drawing operation. Consequently, all parametric studies were carried out using this element type. Figure 3 shows the effect of the die semi angle (α) on the drawing load required for the plastic deformation process. The die semi angle used for the simulation is in the range $1 \leq \alpha \leq 15$ which covers the range used by Neves et al [6] who numerically simulated the variation of drawing stress with die angle using die semi angle in the range $2 \leq \alpha \leq 15$ using the upper bound method.

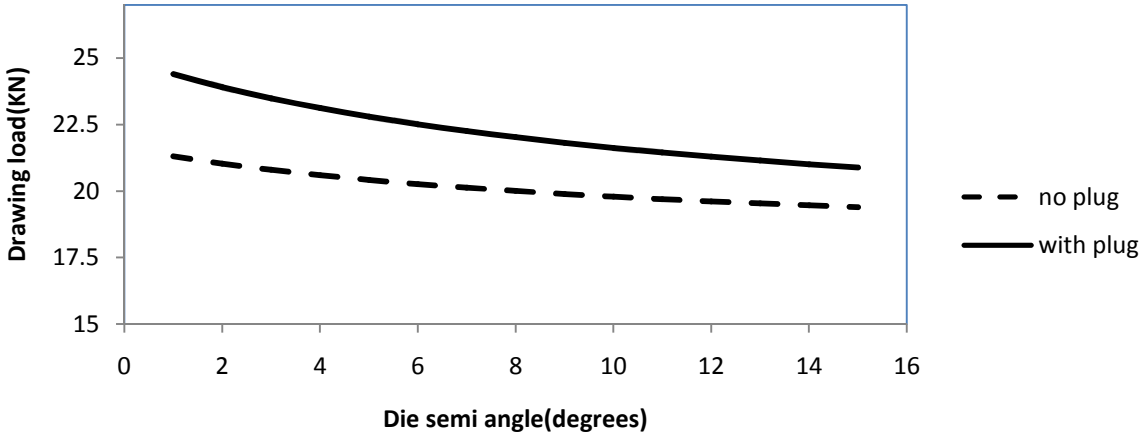

Figure 3: Variation of drawing load with semi die angle for different values of die semi angle.

The base parameters used for the simulation are $\sigma_0 = 1.4 kN/mm^2$, $\beta = 10^0$, and a mesh of six C^0 cubic isoparametric elements. The simulation was carried out for two sets of friction coefficients between the die-tube and plug-tube interfaces. Figure 3 shows the variation of drawing load as a function of die semi angle for die – tube coefficient of friction (μ_1) equal 0.05 and plug – tube coefficient of friction (μ_2) equal 0, representing tube drawing without a plug and coefficient of friction equal 0.05 at both interfaces representing a tube drawing process with a conical die. It can be observed that the drawing load increases with increasing friction between the die – tube interface and plug – tube interface. This finding is consistent with the finding put forward by Neves et al [1] who applied the upper bound method to analyze the tube drawing process. For a cylindrical plug $\beta = 0$. Figure 4 shows the variation of drawing load with die semi angle for tube drawing process with a cylindrical plug ($\beta=0$) and conical plug using the following parameters $\sigma_0 = 1.4 kN/mm^2$, $1^0 \leq \alpha \leq 14^0$, $\mu_1 = 0.05$, $\mu_2 = 0.05$ and a mesh of six C^0 cubic isoparametric elements for the simulation. The conical plug was simulated with two instances of semi angle of the plug namely 6^0 and 8^0.

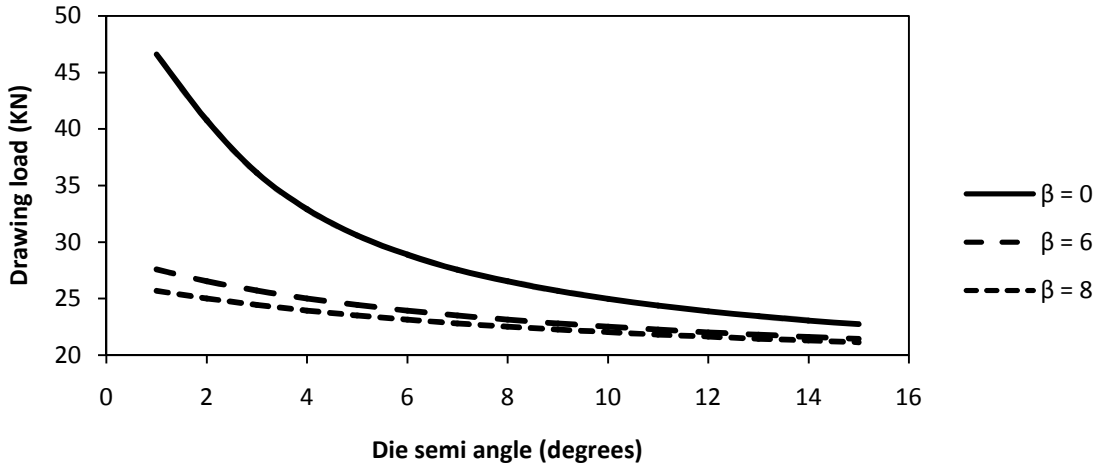

Figure 5: Variation of drawing load with die semi angle for different semi angle of plug.

Figure 5 shows that the drawing load required to produce 84% reduction in area equivalent to drawing a tube of 16mm outside diameter and 1.5mm thickness to 11mm outside diameter and 1mm thickness is greatest when drawn with a cylindrical plug. The drawing load is observed to decrease with increase in the plug – tube semi angle for a given tube – die semi angle. However, the increase in drawing load with decrease in plug – tube semi angle for a given die semi angle is greater for lower die semi angles. It may be concluded from the forgoing that the work done and consequently power requirement needed for tube drawing operation increases with decrease in plug – tube semi angle for a given drawing speed.

Figure 6 shows the comparison of drawing load for tube drawing with a cylindrical moving mandrel and a cylindrical plug under similar conditions. Specifically, the following instance of process parameters were used for the simulation σ_0 = 1.4kN/mm^2, $1^0 \leq \alpha \leq 14^0$, $\mu_1 = 0.05$, μ_2=0.05 and a mesh of six C^0 cubic isoparametric

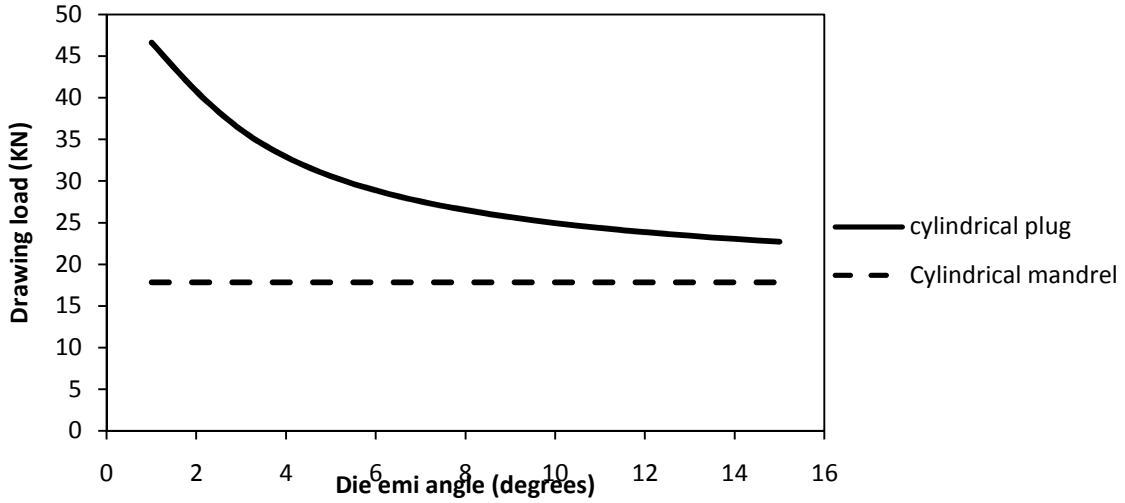

Figure 6: Drawing load as a function of die semi angle for tube drawing with cylindrical plug and cylindrical mandrel

Numerical computation shows that for a given die – tube semi angle, a greater drawing load is required for tube drawing with a cylindrical plug than with a cylindrical mandrel. In addition, for tube drawing with a moving mandrel, the drawing load is independent of the die semi angle and depends only on the flow stress (σ_0) and the percent reduction in tube wall thickness from the entry to the exit. This finding is consistent with result derived from analytical solution of the tube drawing process with moving mandrel. The reason for this behaviour is that in a tube drawing process with moving mandrel, the friction force at the mandrel – tube interface is directed towards the exit of the die and since for a tube drawing process with moving mandrel, the die – tube and tube – mandrel interfaces coefficients of friction are typically identical, the value of the parameter B reduces to zero.

CONCLUSION

A numerical study using the finite element method has been used to analyze the tube drawing operation. The equation governing the elastoplastic deformation process has been derived and solved using the finite element method. The solution obtained using the present method has been shown to be admirably close to the analytical solution with mesh refinement using C^0 cubic isoparametric elements. Parametric studies have been carried out and the effect of die semi angle on drawing load has been presented for tube drawing operation with and without plug and with a moving mandrel. It has been shown that drawing load decreases with die semi angle. This finding is corroborated by studies carried out by Nevas et al [1] who obtained similar results from experimental and numerical analysis of tube drawing. Comparison has also been made between the different tube drawing operations based on drawing load.

REFERENCES

[1]. F.O.,Neves, S.T., Button, C., Caminaga and F.C.,Gentile, Numerical and experimental analysis of tube drawing with a fixed plug, Journal of the Brazilian Society of Mech. Sci. & Eng, vol 27, issue 4, (2005),pp 426 – 431

[2]. N., Alexandrova, Analytical treatment of tube drawing with a mandrel", Journal of Mechanical Engineering Science, vol. 215m number 6, (2001), pp. 581 – 589.

[3]. R., Bihamta, M., Fafard, G., D'Amours, A., Rahem and M., Guillot, Numerical studies on the production of variable thickness aluminum tubes for transportation purposes, SAE 2010 World congress and exhibition, 2010.

[4]. W.P.,Fisher and A.T., Day, A study of the factors controlling the tube sinking process for polymer materials, Journal of Materials Processing Technology, vol. 68, issue 2, (1999),pp. 158 – 162.

[5]. M.I., Panhwar, R., Crampton and M.S.J., Hashmi, Analysis of the tube sinking process based on non Newtonian characteristics of the fluid medium, Journal of Materials Processing Technology, vol. 21, issue 2, (1990), pp. 156 – 175.